

New insight into the exotic states strongly coupled with the $D\bar{D}^*$ from the T_{cc}^+

Guang-Juan Wang,^{1,*} Zhi Yang,^{2,†} Jia-Jun Wu,^{3,‡} Makoto Oka,^{4,5,§} and Shi-Lin Zhu^{6,¶}

¹*KEK Theory Center, Institute of Particle and Nuclear Studies (IPNS), High Energy Accelerator Research Organization (KEK), 1-1 Oho, Tsukuba, Ibaraki, 305-0801, Japan*

²*School of Physics, University of Electronic Science and Technology of China, Chengdu 610054, China*

³*School of Physical Sciences, University of Chinese Academy of Sciences (UCAS), Beijing 100049, China*

⁴*Advanced Science Research Center, Japan Atomic Energy Agency, Tokai, Ibaraki, 319-1195, Japan*

⁵*Nishina Center for Accelerator-Based Science, RIKEN, Wako 351-0198, Japan*

⁶*School of Physics and Center of High Energy Physics, Peking University, Beijing 100871, China*

(Dated: June 22, 2023)

We have investigated the internal structure of the open- and hidden-charmed ($DD^*/\bar{D}\bar{D}^*$) molecules in the unified framework. We first fit the experimental lineshape of the T_{cc}^+ state and extract the DD^* interaction, from which the T_{cc}^+ is assumed to arise solely. Then we obtain the $D\bar{D}^*$ interaction by charge conjugation. Our results show that the $D\bar{D}^*$ interaction is attractive but insufficient to form $X(3872)$. Instead, its formation requires the crucial involvement of the coupled channel effect between the $D\bar{D}^*$ and $c\bar{c}$ components, although the $c\bar{c}$ accounts for approximately 1% only. Besides $X(3872)$, we have obtained a higher-energy state around 3957.9 MeV with a width of 16.7 MeV, which may be a potential candidate for the $X(3940)$. In $J^{PC} = 1^{+-}$ sector, we have found two resonances related to the iso-vector Z_c and the iso-scalar $h_c(2P)$, respectively. Our combined study provides valuable insights into the nature of these $DD^*/D\bar{D}^*$ exotic states.

The exotic states, which are beyond the simple quark model pictures of the quark-antiquark meson and three-quark baryon, have greatly enriched the hadron spectroscopy. Their inner structures remain a mystery and the investigations of their dynamics have been an ongoing and central issue in the study of nonperturbative Quantum Chromodynamics (QCD).

One of the most well-known exotic states is the $X(3872)$ with $J^{PC} = 1^{++}$ (also named as $\chi_{c1}(3872)$ in RPP [1]), which was first observed by the Belle Collaboration in 2003 [2] and subsequently confirmed by various experimental collaborations [3–8]. It is located extremely near the $D^0\bar{D}^{*0}$ ¹ threshold, with a mass difference of $M_{X(3872)} - M_{D^0\bar{D}^{*0}} = 0 \pm 0.18$ MeV. The location is also not too far away from the $\chi_{c1}(2P)$ meson predicted by the Godfrey-Isgur (GI) relativized quark model [9], with $M_{\chi_{c1}(2P)} - M_{X(3872)} = 81.4$ MeV. So far, there are different theoretical interpretations, such as the conventional twisted $\chi_{c1}(2P)$ charmonium [10, 11], the compact tetraquark state [12, 13], the $D^*\bar{D}/D\bar{D}^*$ molecule [14–17], the mixture of the $c\bar{c}$ and $D^*\bar{D}/D\bar{D}^*$ molecule [18–24]. For more details, see Refs. [25–28] for reviews.

The close proximity of the $X(3872)$ makes its nature hidden under the threshold effects with the complexity of the coupled channel effect between the $c\bar{c}$ core and $D\bar{D}^*$ components. Typically, the parameters of the $D\bar{D}^*$ interaction estimated with phenomenological models suffer a large uncertainty because of the limited experimental information. There are two production mechanisms in the molecular model, either an accidental fine-tuning of the parameters associated with the $D\bar{D}^*$ sector or an ac-

idental fine-tuning of a P-wave $c\bar{c}$ meson to the $D\bar{D}^*$ threshold [18].

Recently, the LHCb collaboration reported the observation of the T_{cc}^+ state extremely close to the $D^{*+}D^0$ threshold [29, 30]. The T_{cc}^+ has attracted a great deal of interest [31–53]. Since the T_{cc}^+ is observed in the $D^0D^0\pi^+$ channel, just below the D^0D^{*+} threshold within several hundreds keV, the DD^* interaction definitely plays the most important role in the formation of this exotic state. Thus, it provides the precious experimental data to constrain the DD^* interaction, which are related to the $D\bar{D}^*$ interaction through charge conjugation. Once $D\bar{D}^*$ interaction is well constrained, the inner structure of the $X(3872)$ can be disentangled. Such combined studies incorporating as many constraints as possible are essential to gain a deeper understanding of the exotic states and shed light on their intricate properties.

The main goal of this Letter is to identify the contributions of the $c\bar{c}$ core and $D\bar{D}^*$ component in the $X(3872)$ in an unambiguous way. We first perform a fit of the T_{cc}^+ spectral function in the one-boson-exchange (OBE) framework and determine the relatively long-range $DD^*/D\bar{D}^*$ interactions with little ambiguity thanks to the precision data. Then charge conjugation symmetry is applied to achieving a systematic and consistent study of multiple exotic states $X(3872)$, T_{cc} and Z_c within the molecular picture. In addition, the $c\bar{c}$ core of the $X(3872)$ and $h_c(2P)$ ($J^{PC} = 1^{+-}$) is included for the complete model, where we describe the transition by the quark-pair creation (QPC) model. The interconnection of these states can help us to reduce the theoretical uncertainties and disentangle the intricate properties of the exotic states. Thus we determine the structure and components of the $X(3872)$, in particular the role of $c\bar{c}$ core

¹ Hereafter, we use the notion $D\bar{D}^*$ to represent $DD^* + c.c.$.

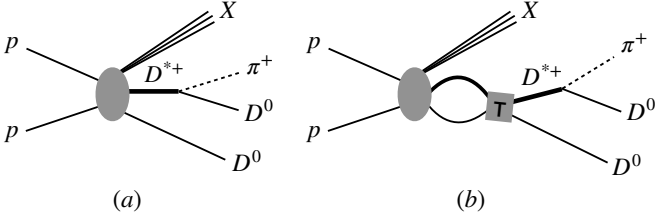


FIG. 1. The Feynman diagram for $pp \rightarrow D^0D^0\pi^+X$ (X denotes all the produced particles other than the D^0 , D^0 and π^+ in the collision). The square labeled as T denotes the scattering T -matrix for the D^0D^{*+} and $D^{*+}D^{*0}$ channels.

and its coupling to $D\bar{D}^*$ component with little ambiguity. We finally make testable predictions of higher $\chi_{c1}(2P)$ and $h_c(2P)$ resonance states, which will provide critical benchmarks for the validity of the theory, and strong motivation for future experimental investigations.

We first concentrate on the $DD^*/D\bar{D}^*$ interaction. The S-wave DD^* and $D\bar{D}^*$ may form the molecules with the spin-parity $J^{P(C)} = 1^{+(\pm)}$ with $I = 1, 0$, as listed in Table I. In the following, we simultaneously study the rel-

atively long-range $DD^*/D\bar{D}^*$ interactions by exchanging the light mesons. We focus on the light pseudoscalar (P) meson π - and vector (V) meson ρ/ω -exchange potentials for the $DD^*/D\bar{D}^*$, while the σ - and η -contribution are neglected due to their tiny contributions [17, 54, 55]. The interactions are derived using the Lagrangians given in Refs. [17, 54] based on heavy quark symmetry. The DD^* and $D\bar{D}^*$ interactions are related to each other using the charge conjugation.

The DD^* and $D\bar{D}^*$ potentials by exchanging the light-meson under the isospin bases are summarized in Table I. The potentials V_π , $V_{\rho/\omega}^u$ and $V_{\rho/\omega}^t$ are given in terms of three coupling constant $g(D^*DP)$, $\lambda(D^*DV)$, and $\beta(DDV/D^*D^*V)$, respectively, as shown in the Supplemental Material. The constant $g = 0.57$ is determined from the strong decay width of $D^* \rightarrow D\pi$ [1].

Subsequently, we determine the above $DD^*/D\bar{D}^*$ interaction by fitting the experimental T_{cc}^+ spectral function with the contributions from the D^0D^{*+} and $D^{*0}D^+$ channels. The inclusive production of the T_{cc}^+ in the $pp \rightarrow D^0(p_{D_1})D^0(p_{D_2})\pi^+(p_\pi)X$, will be interpreted with two mechanisms, as depicted in Fig. 1. The amplitude reads

$$i\mathcal{M}_{pp \rightarrow DD\pi X} = \mathcal{A}_{pp \rightarrow DD^*X}^\mu \left\{ g_{\mu\alpha} - \frac{i}{(2\pi)^4} \int d^4 q_{D^*} G_{D^*\mu\nu}(q_{D^*}) G_D(p_{D_1} + p_{D_2} + p_\pi - q_{D^*}) T_\alpha^\nu(q_{D^*}, p_{D_1} + p_\pi) \right\} \\ \times G_{D^*}^{\alpha\beta}(p_{D_2} + p_\pi)(g_{\mu\beta} + (p_{D_1} \rightarrow p_{D_2})), \quad (1)$$

where $\mathcal{A}_{pp \rightarrow DD^*X}^\mu$ is the production vertex $pp \rightarrow DD^*X$. In the energy region close to the threshold, we consider the S -wave DD^* production contribution only. We have explored both the iso-vector and iso-scalar assignment for the \mathcal{A} with the production amplitudes satisfying $\mathcal{A}_{pp \rightarrow D^+D^{0*}X}^\mu = \pm \mathcal{A}_{pp \rightarrow D^0D^{*+}X}^\mu$, respectively. We are able to find a satisfactory fit to the experimental data only in the iso-scalar case. The G_H is the propagator of the heavy meson H . The DD^* scattering amplitude $T(p_{D^*}, p'_{D^*}) \equiv \epsilon_\mu^*(p_{D^*}) T^{\mu\nu}(p_{D^*}, p'_{D^*}) \epsilon_\nu(p'_{D^*})$ with ϵ the polarization vector, can be solved from the relativistic Lippmann-Schwinger equation [56–59],

$$T(\vec{p}_{D^*}, \vec{p}'_{D^*}; E) = \mathcal{V}(\vec{p}_{D^*}, \vec{p}'_{D^*}; E) + \int d\vec{q} \\ \times \frac{\mathcal{V}(\vec{p}_{D^*}, \vec{q}; E) T(\vec{q}, \vec{p}'_{D^*}; E)}{E - \sqrt{m_D^2 + q^2} - \sqrt{m_{D^*}^2 + q^2} + i\epsilon}. \quad (2)$$

In our calculation, the D^0D^{*+} and $D^{*+}D^{*0}$ are two independent channels. Thus the T and \mathcal{V} -matrix are both 2×2 matrices. The effective potential \mathcal{V} is obtained with the light-meson exchange potentials which incorporates

a form factor to ensure regularization and convergence,

$$\mathcal{V} = \left(V_\pi + V_{\rho/\omega}^t + V_{\rho/\omega}^u \right) \left(\frac{\Lambda^2}{\Lambda^2 + p_f^2} \right)^2 \left(\frac{\Lambda^2}{\Lambda^2 + p_i^2} \right)^2, \quad (3)$$

where Λ is the cut-off parameter. It should be noted that the final results are independent of the specific value of Λ since its dependence can be absorbed into the coupling constants λ and β . To confirm this, we perform fitting procedures with three values $\Lambda = 0.8, 1.0$, and 1.2 GeV, respectively. Our final results remain unchanged regardless of the chosen Λ value. When the cutoff $\Lambda = 1.0$ GeV is taken, the fitted parameters are

$$\lambda = 0.683 \pm 0.025 \text{ /GeV}, \quad \beta = 0.687 \pm 0.017. \quad (4)$$

with $\chi^2/\text{d.o.f.} = 0.78$. The fitted line shape is shown in Fig. 2, together with the line shape before the convolution with the energy resolution function [30].

To identify T_{cc}^+ and explore other possible resonant states while obtaining the wave function, we search the poles in the complex plane using T -matrix pole analysis and complex scaling method (CSM) [60–62], which is introduced in the Supplemental Material. The results are consistent with each other on the bound and resonant

TABLE I. The D^*D and $\bar{D}^*\bar{D}$ interactions in the one-boson-exchange model in the isospin symmetry limit. To facilitate comparison, we have employed the potential forms (D^*D interactions) to express both D^*D and $\bar{D}^*\bar{D}$ interactions, denoted as $V_\phi^{u/t}$ where the subscript ϕ may be π, ρ, ω . The C-parity of the flavor wave functions (neutral system) $[D\bar{D}^*] = \frac{1}{\sqrt{2}}(D\bar{D}^* - D^*\bar{D})$ and $\{D\bar{D}^*\} = \frac{1}{\sqrt{2}}(D\bar{D}^* + D^*\bar{D})$ are even and odd, respectively, using the charge conjugation convention $D^* \rightarrow -\bar{D}^*$ from Ref. [15].

	wave function	$I(J^{PC})$	u – channel : π	u – channel : ρ/ω	t – channel : ρ/ω
DD^*	$\frac{1}{\sqrt{2}}(D^+D^{*0} - D^0D^{*+})$	$0(1^+) [T_{cc}^+]$	$\frac{3}{2}V_\pi$	$\frac{3}{2}V_\rho^u - \frac{1}{2}V_\omega^u$	$-\frac{3}{2}V_\rho^t + \frac{1}{2}V_\omega^t$
	$\frac{1}{\sqrt{2}}(D^+D^{*0} + D^0D^{*+})$	$1(1^+)$	$\frac{1}{2}V_\pi$	$\frac{1}{2}V_\rho^u + \frac{1}{2}V_\omega^u$	$\frac{1}{2}V_\rho^t + \frac{1}{2}V_\omega^t$
$D\bar{D}^*$	$\frac{1}{\sqrt{2}}([D^+D^{*-}] + [D^0\bar{D}^{*0}])$	$0(1^{++}) [X(3872)]$	$\frac{3}{2}V_\pi$	$-\frac{3}{2}V_\rho^u - \frac{1}{2}V_\omega^u$	$-\frac{3}{2}V_\rho^t - \frac{1}{2}V_\omega^t$
	$\frac{1}{\sqrt{2}}([D^+D^{*-}] - [D^0\bar{D}^{*0}])$	$1(1^{++})$	$-\frac{1}{2}V_\pi$	$\frac{1}{2}V_\rho^u - \frac{1}{2}V_\omega^u$	$\frac{1}{2}V_\rho^t - \frac{1}{2}V_\omega^t$
	$\frac{1}{\sqrt{2}}(\{D^+D^{*-}\} + \{D^0\bar{D}^{*0}\})$	$0(1^{+-}) [h_c]$	$-\frac{3}{2}V_\pi$	$\frac{3}{2}V_\rho^u + \frac{1}{2}V_\omega^u$	$-\frac{3}{2}V_\rho^t - \frac{1}{2}V_\omega^t$
	$\frac{1}{\sqrt{2}}(\{D^+D^{*-}\} - \{D^0\bar{D}^{*0}\})$	$1(1^{+-}) [Z_c(3900)]$	$\frac{1}{2}V_\pi$	$-\frac{1}{2}V_\rho^u + \frac{1}{2}V_\omega^u$	$\frac{1}{2}V_\rho^t - \frac{1}{2}V_\omega^t$

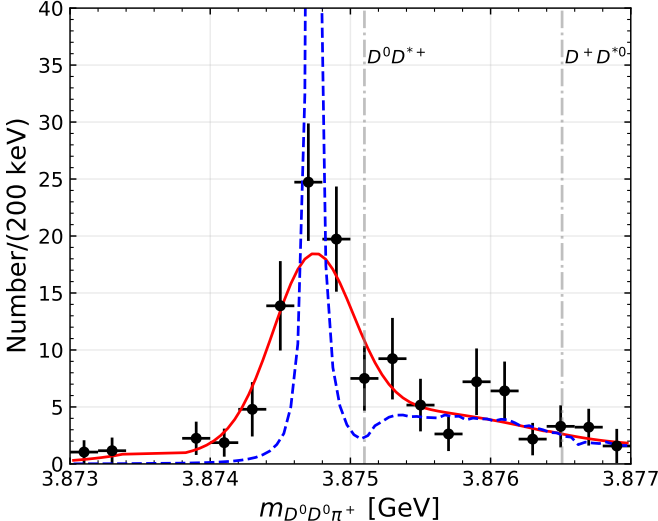


FIG. 2. The fitted lineshape of the T_{cc}^+ in the $D^0D^0\pi^+$ invariant mass spectrum [29]. The blue dashed and red solid lines represent the lineshapes before and after the convolution with the energy resolution function, which is taken from the LHCb collaboration [30].

states. Our results clearly show a distinct signal corresponding to the bound state of the DD^* . We summarize its properties including the mass, decay width, root mean square radius and proportions of different components in Table II. The binding energy of the bound state is $\Delta E = -393.0$ keV, which is consistent with that of the experiment $\Delta E_{\text{exp}} = -360(40)$ keV [30]. In our model, the whole calculation is conducted in the momentum space and the on-shell contribution is included, which naturally generates the width of the T_{cc}^+ around 70 keV through the decay into the $DD\pi$ final state.

The wave function of T_{cc}^+ is presented in Fig. 3. As a shallow S-wave bound state, there is a long tail for

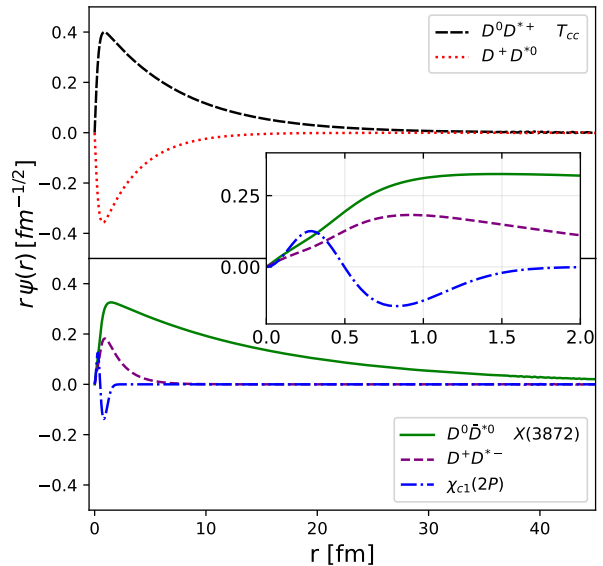


FIG. 3. The wave function distribution of different components for the T_{cc}^+ and $X(3872)$.

the radius distribution. The root mean square radius is around 4.7 fm which establishes the T_{cc}^+ as a molecular state of the DD^* . The ratio of the residue of the $D^{*+}D^0$ and D^+D^{*0} channels is close to 1, showing the similar couplings of the T_{cc}^+ to these two components. Then the difference between the wave functions of two channels is mainly due to their mass difference of 1.4 MeV. Such small mass splitting still introduces a sizeable isospin breaking effect because of its extremely small binding energy, and the iso-vector component occupies around 4.2% in T_{cc}^+ as shown in Table II.

TABLE II. The properties of the T_{cc}^+ and $X(3872)$ in the fit with $\Lambda = 1.0$ GeV. The script ‘‘BE’’ denotes the binding energy. The ratio of the residue in two channels is listed in the last column. For $X(3872)$, the QPC parameter $\gamma = 4.69$.

T_{cc}^+	BE (keV)	Γ (keV)	$\sqrt{\langle r^2 \rangle}$	$I = 0$	$I = 1$	$P(D^0 D^{*+})$	$P(D^+ D^{*0})$	$ \frac{\text{Res}(D^0 D^{*+})}{\text{Res}(D^+ D^{*0})} $
	-393.0	70.4	4.7 fm	95.8%	4.2%	70.0%	30.0%	1.055
$X(3872)$	BE (keV)	Γ (keV)	$\sqrt{\langle r^2 \rangle}$	$I = 0$	$I = 1$	$P(D^0 \bar{D}^{*0})$	$P(D^+ D^{*-})$	$P(c\bar{c})$
	-80.4	32.5	11.2 fm	71.9%	28.1%	94.0%	4.8%	1.2%

The successful interpretation of the T_{cc}^+ encourages us to study the molecular states in the $D\bar{D}^*$ sector composed of the $\bar{D}^0 D^{*0}$ and $D^+ D^{*-}$. With the DD^* interactions, we derive the $D\bar{D}^*$ interactions through the charge conjugation. Then in the $J^{PC} = 1^{++}$ sector where the $X(3872)$ exists, we do not find any bound or virtual states. Interestingly, if we introduce a scaling factor (> 1), for example 1.15, to all couplings of the $D^* \bar{D}$ potentials, a bound state appears with a binding energy 25 keV. This indicates that the $D\bar{D}^*$ interaction is attractive but not strong enough to produce a bound state. The conclusion remains the same using the different cut off value such as 0.8 or 1.2 GeV. Moreover, the bound state can be obtained by fine-tuning the coupling strength in the OBE model as shown above. Therefore the constraint from the T_{cc}^+ is indispensable to study the formation mechanism of the $X(3872)$.

In fact, the $D\bar{D}^*$ system with the quantum numbers $I(J^{PC}) = 0(1^{++})$ can couple with the $\chi_{c1}(2P)$. In the following, we demonstrate that the inclusion of the bare $c\bar{c}$ core is essential to form the $X(3872)$. The mass and wave functions of $\chi_{c1}(2P)$ are determined by using the GI model with the updated parameters from our previous works [63, 64]. To account for the coupled channel effect between the $c\bar{c}$ core and $D\bar{D}^*$, we employ the quark-pair-creation (QPC) model. Within the framework, a light quark pair with the spin-parity $J^{PC} = 0^{++}$ is created and combined with the $c\bar{c}$ pair to form the $D\bar{D}^*$ state. This approach provides a feasible connection between the quark and hadron level. The transition potential reads [65–71],

$$g_{D\bar{D}^*, c\bar{c}}(|\vec{k}_{D\bar{D}^*}|) = \gamma I_{D\bar{D}^*, c\bar{c}}(|\vec{k}_{D\bar{D}^*}|), \quad (5)$$

where $\vec{k}_{D\bar{D}^*}$ is the relative momentum in the $D\bar{D}^*$ channel. $I_{D\bar{D}^*, c\bar{c}}(|\vec{k}_{D\bar{D}^*}|)$ is the overlap of the meson wave functions. The parameter γ represents the amplitude of producing the light quark pair. We choose $\gamma = 4.69$ so that it reproduces the mass and decay of $\psi(3770)(\rightarrow D\bar{D})$ resonance. Using the CSM method, our results show a clear signal of a bound state associated with the $X(3872)$ with a binding energy $\Delta E = -80.4$ keV and a resonant state corresponding to a dressed $c\bar{c}$ state with $J^{PC} = 1^{++}$.

In Table II, we summarize the properties of $X(3872)$. Its width, 32.5 keV, arises predominantly from the decay into the $D^0 \bar{D}^0 \pi^0$ channel. The dominant component

of the $X(3872)$ is the loosely bound molecular state of the neutral $D^0 \bar{D}^{*0}$ (94.0%) and charged $D^+ \bar{D}^{*-}$ (4.8%). The mass difference of 8 MeV between the charged and neutral channels leads to an important isospin breaking for a bound state extremely close to the neutral channel. It is worth highlighting that the $c\bar{c}$ component is crucial to form the $X(3872)$, even though it only accounts for 1.2%.

To visualize the contribution of the $c\bar{c}$, $D^+ D^{*-}$ and $D^0 \bar{D}^{*0}$ components in the $X(3872)$, we display their wave functions in the lower and middle panels of Fig. 3. We employ the $c\bar{c}$ wave function from the GI model, combining with its probability amplitude in the $X(3872)$.

In the short-range region up to 2 fm (middle panel of Fig. 3), both the $c\bar{c}$ and DD^* components are significant. Notably, for $r < 0.5$ fm, the $c\bar{c}$ core dominates. The wave functions show that the main component $D\bar{D}^*$ definitely plays the dominant role in the long-distance region, which contributes to the large size of the $X(3872)$ whose radius around 11.2 fm. This is reasonable because the $X(3872)$ has such a tiny binding energy and couples strongly with the $D\bar{D}^*$ channel.

The isospin-breaking decays $X(3872) \rightarrow J/\psi \omega / \rho$ is attributed to the overlap factor of the wave functions $\int d\vec{p} \psi_{X(3872)}^{I=1/0}(\vec{p}) \psi_{J/\psi}^*(\vec{p})$ in the amplitude [18], yielding a ratio $R_{\omega/\rho} = \frac{\mathcal{B}[X \rightarrow J/\psi \omega]}{\mathcal{B}[X \rightarrow J/\psi \rho]} = 21.4$. Using the factorization formulae [72–74], the decay ratio $\frac{\mathcal{B}[X \rightarrow J/\psi \pi^+ \pi^- \pi^0]}{\mathcal{B}[X \rightarrow J/\psi \pi^+ \pi^-]} = R_{\omega/\rho} \times R_2$ is 1.86 and 3.14, with $R_2 \sim \frac{\mathcal{B}(\omega \rightarrow \pi^+ \pi^- \pi^0)}{\mathcal{B}(\rho \rightarrow \pi^+ \pi^-)}$ being 0.087 [72] and 0.147 [73, 74], respectively. The former decay ratio is consistent with the experimental value $1.0 \pm 0.4 \pm 0.3$ [75].

Besides the $X(3872)$, we also find a signal of the resonant state $\chi_{c1}(2P)$ at

$$M = 3957.9 \text{ MeV}, \quad \Gamma = 16.7 \text{ MeV}, \quad (6)$$

which might be identified as the $X(3940)(M = 3942 \pm 9 \text{ MeV} \text{ and } \Gamma = 37^{+27}_{-17} \text{ MeV})$ observed in the $D\bar{D}^*$ channel [76].

In the $J^{PC} = 1^{+-}$ sector, we find a resonance pole around $M = 3882.5$ MeV and $\Gamma = 52.6$ MeV, and a virtual state far away from the physical region. This resonance may correspond to the $Z_c(3900)$. Our larger decay width compared to the experimental value need to be investigated further by taking into account the coupled-channel effects with the $J/\psi \pi$ and $\eta_c \rho$ channels, which is

shown to be significant in Lattice QCD calculations [77–84]. Moreover, we investigate the coupling between the $h_c(2P)$ component and iso-scalar $D\bar{D}^*$ channel. We observe a signal of $h_c(2P)$ whose pole is around $M = 3963.4$ MeV and $\Gamma = 3.1$ MeV.

In this work, we have provided a novel strategy to study the dynamical origin of the $X(3872)$ as a superposition of $D\bar{D}^*$ and $c\bar{c}$. The $D\bar{D}^*$ interaction is determined through the charge conjugation of the DD^* interaction, which is extracted from the fitting of the line shape of the T_{cc}^+ . Thanks to the high precision data of T_{cc} spectral function, the DD^* interaction as well as the $D\bar{D}^*$ interaction are very well determined.

For the $D\bar{D}^*$ system with $J^{PC} = 1^{++}$, we have found that the pure $D\bar{D}^*$ is attractive, but insufficient to form a bound state. The P-wave $c\bar{c}$ core plays a crucial role in the formation of the $X(3872)$, even though its proportion is quite small. Moreover, the wave function of the $X(3872)$ shows that the $D\bar{D}^*$ component has a long tail causes its large radius, while the $c\bar{c}$ is significant at short distances. Additionally, we predict a higher state with $M = 3957.9$ MeV and $\Gamma = 16.7$ MeV, which might be a good candidate for the $X(3940)$. In the $J^{PC} = 1^{+-}$ sector, we have identified two resonances associated with the $Z_c(3900)$ and $h_c(2P)$ state. Confirming both the $X(3940)$ and $h_c(2P)$ with our prediction should serve as the good test for the validity of our theoretical framework.

Notably, this framework can be extended to establish other exotic states, for which no consensus has been reached for their dynamical origins. They often exhibit characteristics that comes from mixings of various dynamical sources. Therefore, it is important and useful to identify and study their dynamics from its relations to the well-understood hadronic states. Such a systematic approach may allow us to unravel the intricate structure of exotic hadronic states, providing a unique and reliable pathway for investigating XYZ particles.

ACKNOWLEDGMENTS

We thank useful discussions and valuable comments from Dote Akinobu, Meng-Lin Du, Jian-Bo Cheng, Rui Chen, Feng-Kun Guo, Zi-Yang Lin, Mao-Jun Yan, Bing-Song Zou. This work is partly supported by the KAKENHI under Grant Nos. 19H05159, 20K03959, and 21H00132 (M.O.), and 23K03427 (M.O. and G.J.W), and by the National Natural Science Foundation of China (NSFC) under Grants Nos. 12275046 (Z.Y.), 12175239 and 12221005 (J.J.W), 11975033 and 12070131001 (S.L.Z.), and by the Natural Science Foundation of Sichuan Province under Grant No. 2022NSFSC1795 (Z.Y.), and by the National Key R&D Program of China under Contract No. 2020YFA0406400 (J.J.W).

SUPPLEMENTAL MATERIAL

Fit details

The differential cross section for the $pp \rightarrow D(p_{D_1})D(p_{D_2})\pi(p_\pi)$ channel reads

$$\begin{aligned} d\sigma_{pp \rightarrow XDD\pi} &= \frac{(2\pi)^4}{4\sqrt{(p_{p_1} \cdot p_{p_2} - m_p^2 m_p^2)}} |\mathcal{M}|^2 d\Phi_{XDD\pi} \\ \frac{d\sigma_{pp \rightarrow XDD\pi}}{dm_{DD\pi}} &\approx 2m_{DD\pi} \int d\sigma_{pp \rightarrow X+DD\pi} B_2 d\Phi_{DD\pi} \\ &\approx 2m_{DD\pi} \int dm_{12} dm_{23} B_2(E; m_{12}, m_{23}), \end{aligned} \quad (7)$$

where p_{p_1} (p_{p_2}) and m_p are the momentum and mass of the initial photon. m_{ij} is defined as $m_{ij}^2 = (p_i + p_j)^2$ with p_i the momutum of D or π in the final state. B_2 is obtained with the \mathcal{M} in Eq. (1),

$$\begin{aligned} |\mathcal{M}|^2 &= |a_{pp \rightarrow DD^*X}|^2 B_2, \\ B_2 &= \sum_{\lambda_X} \epsilon_\mu(p_X, \lambda_X) \epsilon_{\mu'}^\dagger(p_X, \lambda_X) \mathcal{B}\mu \mathcal{B}^{\dagger\mu'}. \end{aligned} \quad (8)$$

To obtain Eq. (7) in the energy region close to the threshold, we have approximated $A_{pp \rightarrow DD^*X}^\mu = a_{pp \rightarrow DD^*X} \epsilon^\mu(p_X, \lambda_X)$ with $a_{pp \rightarrow DD^*X}$ a constant and independent of the polarization. Moreover, the scattering cross section $\sigma_{pp \rightarrow X+DD\pi}$ is a constant since we only concentrate on a small energy range. For a specific channel, the \mathcal{B}_j^μ (the j -th represents the D^*D channels) reads

$$\begin{aligned} \mathcal{B}_j^\mu(p_{12}, p_{23}) &= g \left\{ \frac{-i(p_\pi^\mu - \frac{p_{12}^\mu p_{12} \cdot p_\pi}{m_{D^*}^2})}{p_{12}^2 - m_{D^*}^2 + im_{D^*} \Gamma_{D^*}} \right\}_j \\ &+ \sum_{i=1,2} ig \int dq_{D^*} q_{D^*}^2 \frac{d\Omega_{q_{D^*}}}{4\pi} \frac{\sqrt{2w_{D_2}}}{\sqrt{2w_{D^*}}} \frac{\sqrt{2w_{D_{12}^*}}}{\sqrt{2w_D}} \\ &\times \frac{T_{ij}^{J00}(M, |q_{D^*}|, |p_{12}|)}{(M - w_{D^*}^i) - w_D^i + i\epsilon} \left\{ \frac{\epsilon_a^*{}^\mu(w_{D^*}, q_{D^*}) \epsilon_a(p_{12}) \cdot p_\pi}{p_{12}^2 - m_{D^*}^2 + im_{D^*} \Gamma_{D^*}} \right\}_j \\ &+ (p_{D_1} \rightarrow p_{D_2}). \end{aligned} \quad (9)$$

where the notations are $p_{12} = p_{D_1} + p_\pi$, $p_{23} = p_{D_2} + p_\pi$ and $w_H = m_H^2 + p_H^2$. In the $D\bar{D}^*$ scattering, we only consider the S-wave contribution. The T_{i1}^{J00} is derived after the partial wave decomposition of the $T(\vec{k}_{D^*}, \vec{k}'_{D^*}; E)$ in Eq. (2). The explicit forms of the potentials in construct-

ing the T -matrix read

$$V_\pi = \frac{g^2}{f_\pi^2} \frac{(q \cdot \epsilon_\lambda)(q \cdot \epsilon_{\lambda'}^\dagger)}{q^2 - m_\pi^2}, \quad (10)$$

$$V_{\rho/\omega}^u = -2\lambda^2 g_V^2 \frac{(\epsilon_{\lambda'}^\dagger \cdot q)(\epsilon_\lambda \cdot q) - q^2 (\epsilon_\lambda \cdot \epsilon_{\lambda'}^\dagger)}{q^2 - m_{\rho/\omega}^2}, \quad (11)$$

$$V_{\rho/\omega}^t = \frac{\beta^2 g_V^2}{2} \frac{(\epsilon_\lambda \cdot \epsilon_{\lambda'}^\dagger)}{q^2 - m_{\rho/\omega}^2}. \quad (12)$$

Here we introduce a constant $g_V = 5.8$ to compare our parameters with other values from the phenomenological estimation [17, 54, 55].

The Independence of the cut-off Λ

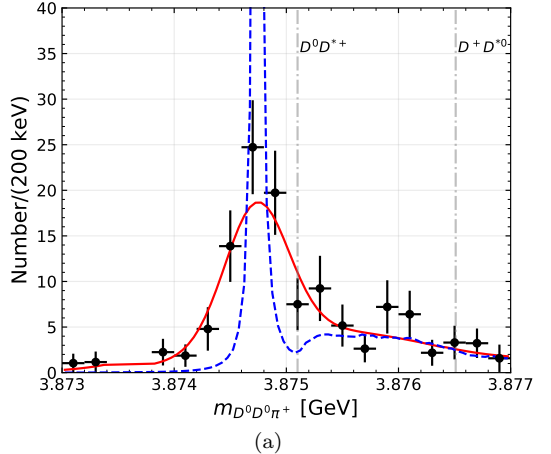
We have used three different values $\Lambda = 0.8, 1.0$, and 1.2 GeV , and obtained the similar fitting results as shown in Figs. 2 and 4. The fitting parameters are

$$\begin{aligned} \lambda_{\Lambda=0.8} &= 0.890 \pm 0.200/\text{GeV}, & \beta_{\Lambda=0.8} &= 0.810 \pm 0.110. \\ \lambda_{\Lambda=1.2} &= 0.587 \pm 0.027/\text{GeV}, & \beta_{\Lambda=1.2} &= 0.550 \pm 0.027. \end{aligned} \quad (13)$$

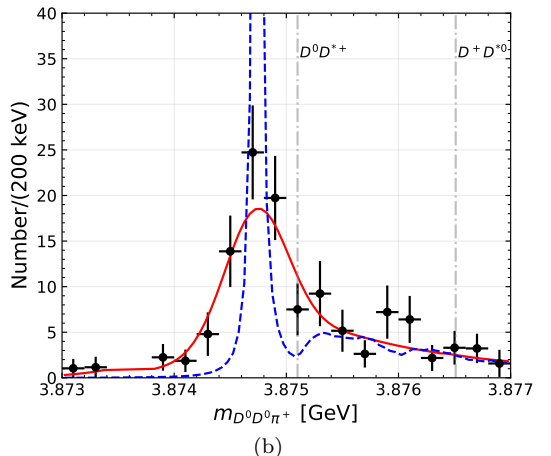
The properties of the T_{cc}^+ with the fitting parameters are summarized in Table III, which clearly shows the independence of the results on the values of the cut-off Λ .

Complex scaling method

The complex scaling method (CSM) is used to identify the bound and resonant states. In CSM, the radius and momentum will rotate with an angle θ , $\mathbf{r} \rightarrow r e^{i\theta}$, $\mathbf{q} \rightarrow \mathbf{q} e^{-i\theta}$. With the varying θ , the scattering states will rotate with 2θ , while the bound and resonant states are independent of the θ and will stay stable. More technical details can be found in Refs. [60–62]. The complex eigenvalues for the DD^* system (T_{cc}) and the DD^* system with $J^{PC} = 1^{++}$ ($X(3872)$) with the parameters in Eq. (4) are displayed Fig. 5.



(a)



(b)

FIG. 4. The fitting results by employing the light-meson-exchanging potential with the cutoff (a) $\Lambda = 0.8 \text{ GeV}$, (b) 1.2 GeV . The $\chi^2/\text{d.o.f.}$ are 0.76 and 0.78, respectively.

- [4] V. M. Abazov et al. (D0), Phys. Rev. Lett. **93**, 162002 (2004), arXiv:hep-ex/0405004.
- [5] B. Aubert et al. (BaBar), Phys. Rev. D **71**, 071103 (2005), arXiv:hep-ex/0406022.
- [6] R. Aaij et al. (LHCb), Eur. Phys. J. C **72**, 1972 (2012), arXiv:1112.5310 [hep-ex].
- [7] R. Aaij et al. (LHCb), Phys. Rev. Lett. **110**, 222001 (2013), arXiv:1302.6269 [hep-ex].
- [8] S. Chatrchyan et al. (CMS), JHEP **04**, 154 (2013), arXiv:1302.3968 [hep-ex].
- [9] S. Godfrey and N. Isgur, Phys. Rev. D **32**, 189 (1985).
- [10] T. Barnes and S. Godfrey, Phys. Rev. D **69**, 054008 (2004), arXiv:hep-ph/0311162.
- [11] Y. S. Kalashnikova and A. V. Nefediev, Phys. Rev. D **82**, 097502 (2010), arXiv:1008.2895 [hep-ph].
- [12] L. Maiani, F. Piccinini, A. D. Polosa, and V. Riquer, Phys. Rev. D **71**, 014028 (2005), arXiv:hep-ph/0412098.
- [13] D. Ebert, R. N. Faustov, and V. O. Galkin, Phys. Lett. B **634**, 214 (2006), arXiv:hep-ph/0512230.
- [14] N. A. Tornqvist, Phys. Lett. B **590**, 209 (2004), arXiv:hep-ph/0402237.
- [15] Y.-R. Liu, X. Liu, W.-Z. Deng, and S.-L. Zhu, Eur. Phys. J. C **56**, 63 (2008), arXiv:0801.3540 [hep-ph].

* wujj@post.kek.jp

† zhiyang@uestc.edu.cn, corresponding author

‡ wujiajun@ucas.ac.cn, corresponding author

§ makoto.oka@riken.jp

¶ zhushl@pku.edu.cn

- [1] R. L. Workman et al. (Particle Data Group), PTEP **2022**, 083C01 (2022).
- [2] S. K. Choi et al. (Belle), Phys. Rev. Lett. **91**, 262001 (2003), arXiv:hep-ex/0309032.
- [3] D. Acosta et al. (CDF), Phys. Rev. Lett. **93**, 072001 (2004), arXiv:hep-ex/0312021.

TABLE III. The properties of the T_{cc}^+ [29] in the three fits with the cutoff values $\Lambda = 0.8, 1.0$, and 1.2 GeV. The script “BE” denotes the binding energy. The ratio of the residue in two channels is listed in the last column.

Λ (GeV)	BE (keV)	Γ (keV)	$\sqrt{\langle r^2 \rangle}$	$I = 0$	$I = 1$	$P(D^0 D^{*+})$	$P(D^+ D^{*0})$	$ \frac{\text{Res}(D^0 D^{*+})}{\text{Res}(D^+ D^{*0})} $
0.8	-387.7	67.3	4.8 fm	95.8%	4.2%	70.0%	30.0%	1.063
1.0	-393.0	70.4	4.7 fm	95.8%	4.2%	70.0%	30.0%	1.055
1.2	-391.6	72.7	4.7 fm	95.7%	4.3%	70.3%	29.7%	1.052

- [16] X. Liu, Z.-G. Luo, Y.-R. Liu, and S.-L. Zhu, Eur. Phys. J. C **61**, 411 (2009), arXiv:0808.0073 [hep-ph].
- [17] N. Li and S.-L. Zhu, Phys. Rev. D **86**, 074022 (2012), arXiv:1207.3954 [hep-ph].
- [18] E. Braaten and M. Kusunoki, Phys. Rev. D **69**, 074005 (2004), arXiv:hep-ph/0311147.
- [19] Y. S. Kalashnikova, Phys. Rev. D **72**, 034010 (2005), arXiv:hep-ph/0506270.
- [20] T. Barnes and E. S. Swanson, Phys. Rev. C **77**, 055206 (2008), arXiv:0711.2080 [hep-ph].
- [21] P. G. Ortega, J. Segovia, D. R. Entem, and F. Fernandez, Phys. Rev. D **81**, 054023 (2010), arXiv:0907.3997 [hep-ph].
- [22] B.-Q. Li, C. Meng, and K.-T. Chao, Phys. Rev. D **80**, 014012 (2009), arXiv:0904.4068 [hep-ph].
- [23] V. Baru, C. Hanhart, Y. S. Kalashnikova, A. E. Kudryavtsev, and A. V. Nefediev, Eur. Phys. J. A **44**, 93 (2010), arXiv:1001.0369 [hep-ph].
- [24] Y. Yamaguchi, A. Hosaka, S. Takeuchi, and M. Takizawa, J. Phys. G **47**, 053001 (2020), arXiv:1908.08790 [hep-ph].
- [25] H.-X. Chen, W. Chen, X. Liu, and S.-L. Zhu, Phys. Rept. **639**, 1 (2016), arXiv:1601.02092 [hep-ph].
- [26] A. Esposito, A. Pilloni, and A. D. Polosa, Phys. Rept. **668**, 1 (2017), arXiv:1611.07920 [hep-ph].
- [27] N. Brambilla, S. Eidelman, C. Hanhart, A. Nefediev, C.-P. Shen, C. E. Thomas, A. Vairo, and C.-Z. Yuan, Phys. Rept. **873**, 1 (2020), arXiv:1907.07583 [hep-ex].
- [28] Y. S. Kalashnikova and A. V. Nefediev, Phys. Usp. **62**, 568 (2019), arXiv:1811.01324 [hep-ph].
- [29] R. Aaij et al. (LHCb), Nature Phys. **18**, 751 (2022), arXiv:2109.01038 [hep-ex].
- [30] R. Aaij et al. (LHCb), Nature Commun. **13**, 3351 (2022), arXiv:2109.01056 [hep-ex].
- [31] S. S. Agaev, K. Azizi, and H. Sundu, Nucl. Phys. B **975**, 115650 (2022), arXiv:2108.00188 [hep-ph].
- [32] X.-Z. Ling, M.-Z. Liu, L.-S. Geng, E. Wang, and J.-J. Xie, Phys. Lett. B **826**, 136897 (2022), arXiv:2108.00947 [hep-ph].
- [33] R. Chen, Q. Huang, X. Liu, and S.-L. Zhu, Phys. Rev. D **104**, 114042 (2021), arXiv:2108.01911 [hep-ph].
- [34] X.-K. Dong, F.-K. Guo, and B.-S. Zou, Commun. Theor. Phys. **73**, 125201 (2021), arXiv:2108.02673 [hep-ph].
- [35] A. Feijoo, W. H. Liang, and E. Oset, Phys. Rev. D **104**, 114015 (2021), arXiv:2108.02730 [hep-ph].
- [36] M.-J. Yan and M. P. Valderrama, Phys. Rev. D **105**, 014007 (2022), arXiv:2108.04785 [hep-ph].
- [37] Q. Xin and Z.-G. Wang, (2021), arXiv:2108.12597 [hep-ph].
- [38] Y. Huang, H. Q. Zhu, L.-S. Geng, and R. Wang, Phys. Rev. D **104**, 116008 (2021), arXiv:2108.13028 [hep-ph].
- [39] S. Fleming, R. Hodges, and T. Mehen, Phys. Rev. D **104**, 116010 (2021), arXiv:2109.02188 [hep-ph].
- [40] K. Azizi and U. Özdem, Phys. Rev. D **104**, 114002 (2021), arXiv:2109.02390 [hep-ph].
- [41] Y. Hu, J. Liao, E. Wang, Q. Wang, H. Xing, and H. Zhang, Phys. Rev. D **104**, L111502 (2021), arXiv:2109.07733 [hep-ph].
- [42] K. Chen, R. Chen, L. Meng, B. Wang, and S.-L. Zhu, Eur. Phys. J. C **82**, 581 (2022), arXiv:2109.13057 [hep-ph].
- [43] M. Albaladejo, Phys. Lett. B **829**, 137052 (2022), arXiv:2110.02944 [hep-ph].
- [44] M.-L. Du, V. Baru, X.-K. Dong, A. Filin, F.-K. Guo, C. Hanhart, A. Nefediev, J. Nieves, and Q. Wang, Phys. Rev. D **105**, 014024 (2022), arXiv:2110.13765 [hep-ph].
- [45] C. Deng and S.-L. Zhu, Phys. Rev. D **105**, 054015 (2022), arXiv:2112.12472 [hep-ph].
- [46] S. S. Agaev, K. Azizi, and H. Sundu, (2022), arXiv:2201.02788 [hep-ph].
- [47] E. Braaten, L.-P. He, K. Ingles, and J. Jiang, Phys. Rev. D **106**, 034033 (2022), arXiv:2202.03900 [hep-ph].
- [48] J. He and X. Liu, Eur. Phys. J. C **82**, 387 (2022), arXiv:2202.07248 [hep-ph].
- [49] L. M. Abreu, H. P. L. Vieira, and F. S. Navarra, Phys. Rev. D **105**, 116029 (2022), arXiv:2202.10882 [hep-ph].
- [50] N. N. Achasov and G. N. Shestakov, Phys. Rev. D **105**, 096038 (2022), arXiv:2203.17100 [hep-ph].
- [51] M. Mikhasenko, (2022), arXiv:2203.04622 [hep-ph].
- [52] B. Wang and L. Meng, (2022), arXiv:2212.08447 [hep-ph].
- [53] Y. Lyu, S. Aoki, T. Doi, T. Hatsuda, Y. Ikeda, and J. Meng, (2023), arXiv:2302.04505 [hep-lat].
- [54] N. Li, Z.-F. Sun, X. Liu, and S.-L. Zhu, Phys. Rev. D **88**, 114008 (2013), arXiv:1211.5007 [hep-ph].
- [55] Q. Wang, V. Baru, A. A. Filin, C. Hanhart, A. V. Nefediev, and J. L. Wynen, Phys. Rev. D **98**, 074023 (2018), arXiv:1805.07453 [hep-ph].
- [56] A. Matsuyama, T. Sato, and T. S. H. Lee, Phys. Rept. **439**, 193 (2007), arXiv:nucl-th/0608051.
- [57] J.-J. Wu, T. S. H. Lee, and B. S. Zou, Phys. Rev. C **85**, 044002 (2012), arXiv:1202.1036 [nucl-th].
- [58] J.-J. Wu, T.-S. H. Lee, A. W. Thomas, and R. D. Young, Phys. Rev. C **90**, 055206 (2014), arXiv:1402.4868 [hep-lat].
- [59] Z.-W. Liu, W. Kamleh, D. B. Leinweber, F. M. Stokes, A. W. Thomas, and J.-J. Wu, Phys. Rev. Lett. **116**, 082004 (2016), arXiv:1512.00140 [hep-lat].
- [60] S. Aoyama, T. Myo, K. Katō, and K. Ikeda, Progress of Theoretical Physics **116**, 1 (2006).
- [61] T. Myo, Y. Kikuchi, H. Masui, and K. Katō, Prog. Part. Nucl. Phys. **79**, 1 (2014), arXiv:1410.4356 [nucl-th].
- [62] N. Moiseyev, Physics reports **302**, 212 (1998).

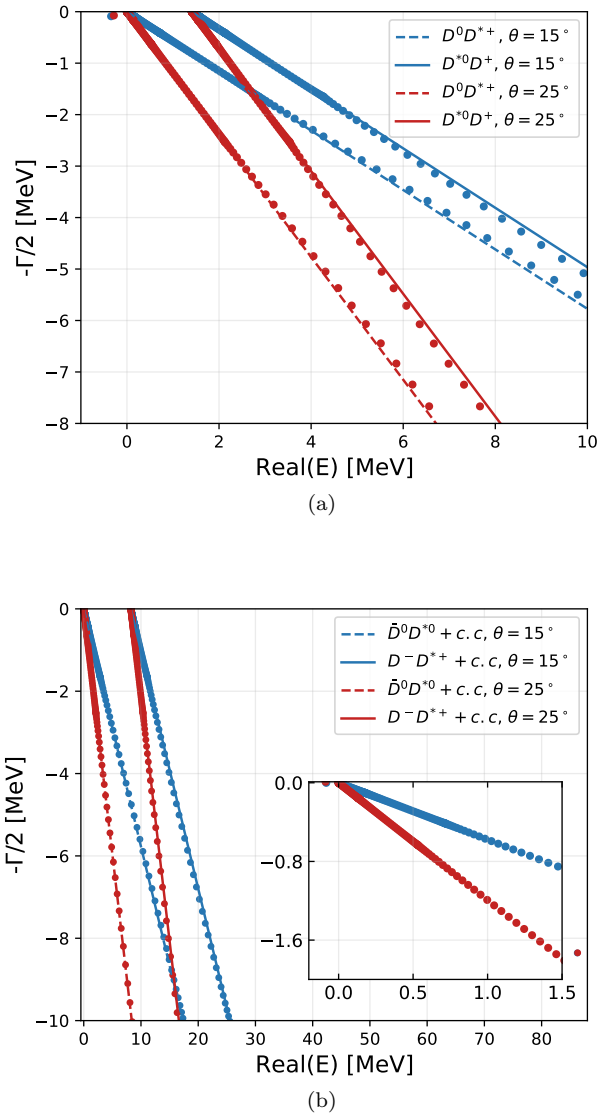


FIG. 5. The complex eigenvalues by employing the light-meson-exchanging potential with the cutoff $\Lambda = 1.0$ GeV in the channels: (a) D^0D^{*+} and $D^{*0}D^+$ channels; (b) $\chi_{c1}(2P)$, \bar{D}^0D^{*0} and D^-D^{*+} channels. The bound states in (a) and (b) correspond to the T_{cc}^+ and $X(3872)$, respectively. The resonant state in (b) is related to the $X(3940)$. The y-axis of the eigenvalues in CSM method corresponds to the half of the decay width.

- [63] Z. Yang, G.-J. Wang, J.-J. Wu, M. Oka, and S.-L. Zhu, Phys. Rev. Lett. **128**, 112001 (2022), arXiv:2107.04860 [hep-ph].
- [64] Z. Yang, G.-J. Wang, J.-J. Wu, M. Oka, and S.-L. Zhu, JHEP **01**, 058 (2023), arXiv:2207.07320 [hep-lat].
- [65] A. Le Yaouanc, L. Oliver, O. Pene, and J. C. Raynal, Phys. Lett. B **71**, 397 (1977).
- [66] R. Kokoski and N. Isgur, Phys. Rev. D **35**, 907 (1987).
- [67] P. R. Page, Nucl. Phys. B **446**, 189 (1995), arXiv:hep-ph/9502204.
- [68] H. G. Blundell, (1996), arXiv:hep-ph/9608473.
- [69] E. S. Ackleh, T. Barnes, and E. S. Swanson, Phys. Rev. D **54**, 6811 (1996), arXiv:hep-ph/9604355.
- [70] D. Morel and S. Capstick, (2002), arXiv:nucl-th/0204014.
- [71] P. G. Ortega, J. Segovia, D. R. Entem, and F. Fernandez, Phys. Rev. D **94**, 074037 (2016), arXiv:1603.07000 [hep-ph].
- [72] E. Braaten and M. Kusunoki, Phys. Rev. D **72**, 054022 (2005), arXiv:hep-ph/0507163.
- [73] D. Gammermann, J. Nieves, E. Oset, and E. Ruiz Arriola, Phys. Rev. D **81**, 014029 (2010), arXiv:0911.4407 [hep-ph].
- [74] L. Meng, G.-J. Wang, B. Wang, and S.-L. Zhu, Phys. Rev. D **104**, 094003 (2021), arXiv:2109.01333 [hep-ph].
- [75] K. Abe et al. (Belle) (2005) arXiv:hep-ex/0505037.
- [76] K. Abe et al. (Belle), Phys. Rev. Lett. **98**, 082001 (2007), arXiv:hep-ex/0507019.
- [77] S. Prelovsek and L. Leskovec, Phys. Lett. B **727**, 172 (2013), arXiv:1308.2097 [hep-lat].
- [78] S. Prelovsek, C. B. Lang, L. Leskovec, and D. Mohler, Phys. Rev. D **91**, 014504 (2015), arXiv:1405.7623 [hep-lat].
- [79] S.-h. Lee, C. DeTar, D. Mohler, and H. Na (Fermilab Lattice, MILC), (2014), arXiv:1411.1389 [hep-lat].
- [80] Y. Chen et al., Phys. Rev. D **89**, 094506 (2014), arXiv:1403.1318 [hep-lat].
- [81] Y. Ikeda, S. Aoki, T. Doi, S. Gongyo, T. Hatsuda, T. Inoue, T. Iritani, N. Ishii, K. Murano, and K. Sasaki (HAL QCD), Phys. Rev. Lett. **117**, 242001 (2016), arXiv:1602.03465 [hep-lat].
- [82] Y. Ikeda (HAL QCD), J. Phys. G **45**, 024002 (2018), arXiv:1706.07300 [hep-lat].
- [83] C. Liu, L. Liu, and K.-L. Zhang, Phys. Rev. D **101**, 054502 (2020), arXiv:1911.08560 [hep-lat].
- [84] T. Chen, Y. Chen, M. Gong, C. Liu, L. Liu, Y.-B. Liu, Z. Liu, J.-P. Ma, M. Werner, and J.-B. Zhang (CLQCD), Chin. Phys. C **43**, 103103 (2019), arXiv:1907.03371 [hep-lat].